

RESEARCH ARTICLE

10.1002/2014JE004666

Key Points:

- Complete survey of Mars' Tharsis region
- Permittivity and loss tangent values of the flows are consistent with basalt
- Used SHARAD data to estimate flow properties

Correspondence to:

M. N. Simon,
msimon@pl.arizona.edu

Citation:

Simon, M. N., L. M. Carter, B. A. Campbell, R. J. Phillips, and S. Mattei (2014), Studies of lava flows in the Tharsis region of Mars using SHARAD, *J. Geophys. Res. Planets*, 119, 2291–2299, doi:10.1002/2014JE004666.

Received 13 MAY 2014

Accepted 26 SEP 2014

Accepted article online 30 SEP 2014

Published online 4 NOV 2014

Studies of lava flows in the Tharsis region of Mars using SHARAD

Molly N. Simon¹, Lynn M. Carter², Bruce A. Campbell³, Roger J. Phillips⁴, and Stefania Mattei⁵

¹Lunar and Planetary Laboratory, University of Arizona, Tucson, Arizona, USA, ²Planetary Geodynamics Laboratory, NASA Goddard Space Flight Center, Greenbelt, Maryland, USA, ³Center for Earth and Planetary Studies, Smithsonian Institution, Washington, District of Columbia, USA, ⁴Planetary Science Directorate, Southwest Research Institute, Boulder, Colorado, USA, ⁵CO.RI.S.T.A., Naples, Italy

Abstract The Tharsis region of Mars is covered in volcanic flows that can stretch for tens to hundreds of kilometers. Radar measurements of the dielectric properties of these flows can provide information regarding their composition and density. SHARAD (shallow radar), a sounding radar on the Mars Reconnaissance Orbiter, detects basal interfaces beneath flows in some areas of Tharsis northwest and west of Ascræus Mons, with additional detections south of Pavonis Mons. Comparisons with 12.6 cm ground-based radar images suggest that SHARAD detects basal interfaces primarily in dust or regolith-mantled regions. We use SHARAD data to estimate the real relative permittivity of the flows by comparing the measured time delay of returns from the subsurface with altimetry measurements of the flow heights relative to the surrounding plains. In cases where the subsurface interface is visible at different depths, spanning tens of meters, it is also possible to measure the loss tangent ($\tan \delta$) of the material. The permittivity values calculated range from 7.6 to 11.6, with an average of 9.6, while the mean loss tangent values range from 7.8×10^{-3} to 2.9×10^{-2} with an average of 1.0×10^{-2} . These permittivity and loss tangent estimates for the flows northwest of Ascræus Mons, west of Ascræus Mons, and south of Pavonis Mons are consistent with the lab-measured values for dense, low-titanium basalt.

1. Introduction

The Tharsis region on Mars is home to the shield volcanoes Arsia, Pavonis, and Ascræus Montes and is covered in volcanic flows that can stretch for tens to hundreds of kilometers. These three volcanoes form a chain between -20° to 20°N and 230° to 260°E . While the surfaces of most of the flows in this region are thought to be young (hundreds of millions of years) based on crater counts, the length of time over which Tharsis developed is unknown and could be either hundreds of millions or billions of years [Bleacher *et al.*, 2007]. Analysis of high-resolution images has shown that flows that are present earlier in the stratigraphic sequence have traveled farther from the volcanoes, while “late stage” flows terminate closer to the volcanoes and originate from rift zones [Bleacher *et al.*, 2007].

The composition of volcanic deposits and lava flows, in addition to type and distribution of volcanic materials, can provide information about the evolution of the surface and interior of a planet. The thickness of the Tharsis area flows varies, but they are typically between 30 and 70 m thick as measured from Mars Orbiter Laser Altimeter (MOLA) data. Physical models propose that they may have been emplaced as individual thick flows traveling over flat, smooth surfaces [Baloga *et al.*, 2003]. These models also suggest that Tharsis area lavas, including flows in close proximity to Ascræus and Pavonis Montes, had viscosities consistent with basaltic composition [Glaze *et al.*, 2009; Baloga and Glaze, 2008; Glaze and Baloga, 2006]. Imaging radar data at 12.6 cm wavelength show extensive, radar-bright flows emanating from the Tharsis Montes [Harmon *et al.*, 2012]. Circular polarization ratios of the radar-bright flows approach unity, suggesting that the surfaces are rough at the centimeter scale to meter scale and that conditions necessary to produce blocky flow surfaces were common on Mars [Harmon *et al.*, 2012].

Sounding radar measurements of the permittivity of volcanic deposits can provide information regarding their composition and density. This information can be used to compare the dielectric properties of lava flows to that of terrestrial or lunar surface materials. Two sounding radars are currently in orbit around Mars: Mars Advanced Radar for Subsurface and Ionosphere Sounding on Mars Express and SHARAD (shallow radar) on the Mars Reconnaissance Orbiter (MRO). Previous measurements of the Medusae Fossae Formation

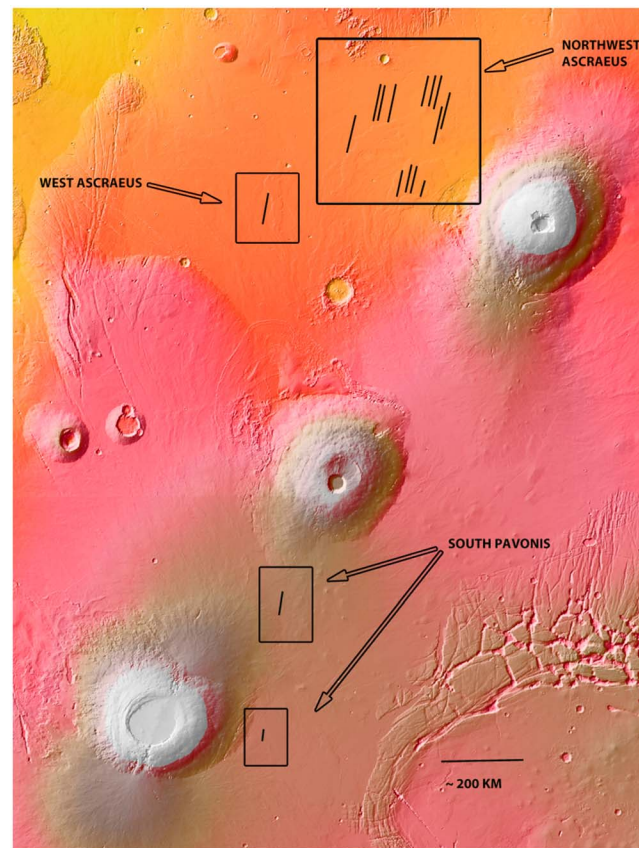


Figure 1. A map of the locations of flow basal interfaces detected by SHARAD in the Tharsis region, shown on MOLA topography. From left to right the orbit track observation numbers northwest of Ascaeus are 1375301, 1297501, 1354201, 1333101, 423301, 1234201, 814901, 189901, 1078601, and 1326501, respectively. Track 1756402 west of Ascaeus Mons and the northern and southern flows along track 1728801 south of Pavonis Mons are also shown above.

tangent given an independent measurement of the flow thickness. Because the Tharsis region is dust covered, the ability of radar to penetrate below the surface is especially useful. The long wavelength of SHARAD (15 m) compared to 12.6 cm imaging radar analysis such as that of *Harmon et al.* [2012] means that the radar is insensitive to centimeter-scale surface roughness and can penetrate surface interfaces that appear rugged in the shorter-wavelength data. In the Tharsis region, relatively flat, smooth, dust-covered surfaces afford ideal conditions for measuring the material properties of these flows. New data from SHARAD provide additional spatial coverage relative to the *Carter et al.* [2009a] results, and we used these data to conduct the first thorough investigation of the entire Tharsis region.

2. Data Analysis: Measurement of Dielectric Properties

SHARAD operates at 20 MHz with a 10 MHz bandwidth and has a free-space vertical resolution of 15 m (~5–10 m vertical resolution in most geologic materials) [*Seu et al.*, 2004]. SHARAD is able to detect permittivity boundaries between thin (tens of meters) layers provided that there is sufficient change in dielectric properties between them. The lateral resolution of SHARAD is 3 to 6 km, reducible to 300 to 1000 m in the “along-track” direction with synthetic aperture focusing [*Seu et al.*, 2004, 2007]. For smooth surfaces, the cross-track resolution is ~3 km [*Seu et al.*, 2007]. SHARAD is sensitive to wavelength-scale topographic features that contribute off-nadir surface clutter to the received echoes. However, the subsurface interfaces discussed below are not visible in surface clutter simulations created using a facet-based, geometric-optics radar model [*Holt et al.*, 2006], and we therefore conclude that they are not clutter.

(MFF), a potential pyroclastic deposit, generated low values (between 3 and 4) for the permittivity and low values (0.001–0.005) for the loss tangent [*Carter et al.*, 2009b; *Heggy et al.*, 2001; *Watters et al.*, 2007]. These values are consistent with values measured for ash and tephra deposits [*Ulaby et al.*, 1988; *Campbell and Ulrichs*, 1969]. In contrast to the low-density MFF materials, permittivity calculations for two flows west of Ascaeus Mons yielded average values of 12.2 and 9.8 for the northern and southern flows, respectively. On Earth, dense basalts have permittivities between 7 and 11 [*Ulaby et al.*, 1988; *Campbell and Ulrichs*, 1969]. The derived permittivity values for the Ascaeus area flows imply densities of 3.4 to 3.7 g cm⁻³. Loss tangent values for these flows range from 0.01 to 0.03 [*Carter et al.*, 2009a]. The measured bulk permittivity and loss tangent values are consistent with those of terrestrial and lunar basalts.

SHARAD is able to determine the permittivity of lava flows, provided that it can detect a subsurface interface. If the radar wave penetrates a lava flow and reflects from a basal interface with material of sufficient dielectric contrast, it is possible to calculate the flow permittivity and loss

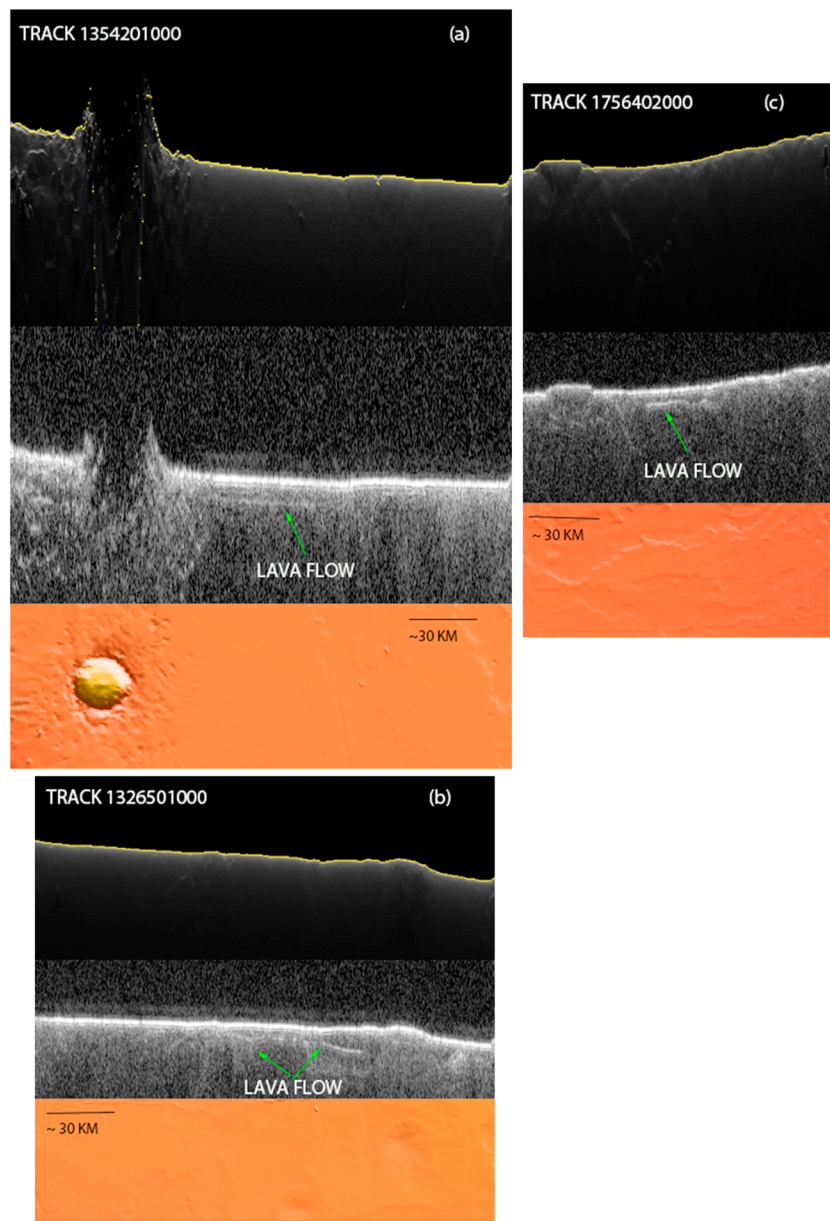


Figure 2. Focused radargrams of orbit tracks 1354201, 1326501, and 1756402 with bright subsurface interfaces visible in the Tharsis region. (a and b) Tracks located northwest of Ascaeus Mons and (c) track located west of Ascaeus Mons. The upper third of the image corresponds to the clutter simulation, confirming that the late time delay echoes in the radargram (middle) are a subsurface interface. The lower third of the figure is the surface topography (MOLA color shaded relief) of the area where the lava flow is located. For track 1354201, we were able to estimate both permittivity and loss tangents values, whereas for track 1756402 we were only able to estimate a loss tangent. For track 1326501, a flow is clearly detected but we were unable to estimate a permittivity or loss tangent value for this particular track.

SHARAD is able to detect subsurface interfaces most clearly north and west of Ascaeus Mons, with additional detections south of Pavonis Mons (Figure 1). Focused radargrams of two of the tracks northwest of Ascaeus Mons and the track west of Ascaeus Mons are shown in Figure 2. For this paper, we reanalyzed the *Carter et al.* [2009a] tracks (423301, 1234201, 814901, 189901, and 1078601) for consistency and error estimation, but we did not repeat the measurements for tracks 423301 and 1234201 since they were already published. For track 1078601, we present results for a northern flow component that was not measured by *Carter et al.* [2009a]. The track 1728801 south of Pavonis Mons has two visible flows along the same track (Figure 3).

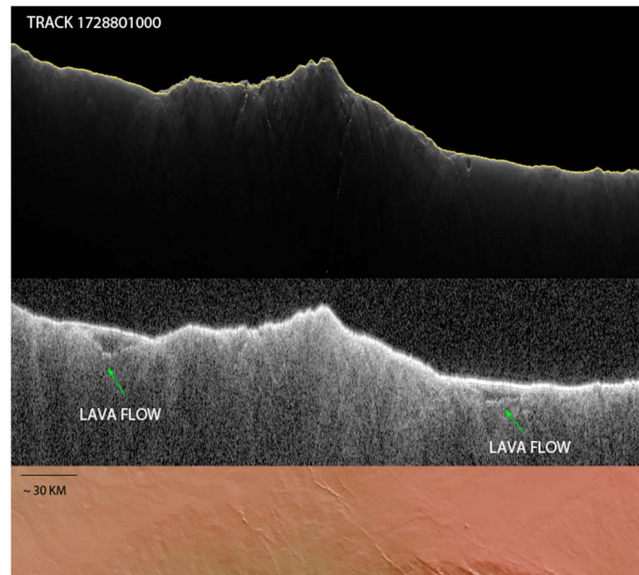


Figure 3. Focused radargram of the orbit track 1728801 located south of Pavonis Mons. An explanation of the upper, middle, and lower third of the image can be found in Figure 2. This track has two visible subsurface interfaces. The lava flow on the left side of the image corresponds to the northern flow while the flow on the right side of the image corresponds to the southern flow.

We can estimate the real relative permittivity of the flows by comparing the measured time delay of returns from the subsurface with altimetry measurements of the flow heights relative to the surrounding plains. The real relative permittivity, denoted by ϵ' , can be calculated from

$$\epsilon' = \left(\frac{c\Delta t}{2h} \right)^2 \quad (1)$$

where h is the height relative to the surrounding plains as measured from MOLA topography and Δt is the two-way time delay between the surface and subsurface echoes measured from the radargram. The relative permittivity is defined as the absolute permittivity divided by the vacuum permittivity. This equation could not be used to derive permittivities for all of the lava flows in the Tharsis region due to an inability to accurately measure h in areas with no surface expression of the

flow. For the lava flows where the real permittivity could be measured, northwest of Ascaeus Mons, ϵ' values ranged from 7.6 to 11.6, with a mean of 9.6 and a standard deviation of 1.9. Pumice, volcanic ash, and tuff have permittivity values between ~ 2.5 and 3, whereas most terrestrial and lunar basalts have ϵ' values between 7 and 11 [Carrier *et al.*, 1991]. The permittivity values calculated for the flows northwest of Ascaeus yield results that most closely resemble basaltic flows. The only plausible way for the real permittivity values to be in the range of felsic (lower density) lavas would be if the flows were sitting in topographic depressions so that the regional projection underestimated h (by just the right amount), which seems unlikely based on the regional topography. For the flows south of Pavonis Mons, the flow west of Ascaeus Mons, and the additional two lava flows northwest of Ascaeus Mons, it was not possible to measure ϵ' , and analysis of these flows is restricted to their loss tangents.

The largest source of error in the real relative permittivity is measurement of the flow height from topography. We assume that the flows sit above a flat surface that is an extension of the surrounding plains, and deviations from this assumption will cause errors. In addition, the subsurface interface time delay values can only be measured within one or two range cells, which causes an additional possible ~ 10 m inaccuracy. We derived 1 sigma errors in the real permittivity by assuming a 2 range bin measurement error on the radargram and a 5 m error on the topographic measurements. The 1 sigma real permittivity errors are displayed in Table 1. However, it is not possible to know whether our initial assumption of a flat subsurface is correct, so these are minimum errors on the calculated values. As an additional test of the accuracy of our permittivity measurements, the orbit tracks in Carter *et al.* [2009a] were independently mapped and measured. The permittivity values were within 2 of those calculated by Carter *et al.* [2009a]. Furthermore, the overall range of permittivities we found was consistent with those of Carter *et al.* [2009a] as well.

In cases where the subsurface interface is visible at different depths, spanning tens of meters, it is also possible to measure the loss tangent ($\tan \delta$) of the material [Campbell *et al.*, 2008]:

$$\tan \delta = \frac{\epsilon''}{\epsilon'} = \sqrt{\left[2^* \left(\frac{\lambda}{4\pi c \Delta t} \ln(L) \right)^2 + 1 \right]^2 - 1} \quad (2)$$

where λ is the SHARAD free-space wavelength of 15 m and L is the power loss per unit of round-trip delay time Δt . Separate fits of power loss versus time delay were made for all orbit tracks with a subsurface

Table 1. Permittivity and Loss Tangent Values, in Addition to Statistical Measurements, Error, and Height Estimates Where Appropriate for Each of the Flows Detected in the Tharsis Region^a

Location	Track Number	Permittivity (ε')	Permittivity 1σ Error on Permittivity	Thickness "h" in Meters	Loss Tangent Mean (tan δ)	Loss Tangent 1σ Error	Slope From Fit	Slope From Error	Slope 1σ Error	Number of Tangent Fit Points
NW Ascræus	1375301	—	—	—	6.3×10^{-3}	3.7×10^{-3} – 8.8×10^{-3}	–3.42	–3.42	1.4	115
NW Ascræus	1297501	9.9	3.58	34	1.2×10^{-2}	5.8×10^{-3} – 1.7×10^{-2}	–6.3	–6.3	3.12	82
NW Ascræus	1354201	7.6	2.29	43	6.1×10^{-3}	3.4×10^{-3} – 8.8×10^{-3}	–3.32	–3.32	1.49	98
NW Ascræus	1333101	7.6	2.67	37	7.8×10^{-3}	5.4×10^{-3} – 1.0×10^{-2}	–4.24	–4.24	1.29	124
NW Ascræus (northern flow)	814901	—	—	—	1.1×10^{-2}	8.9×10^{-3} – 1.4×10^{-2}	–6.25	–6.25	1.4	127
NW Ascræus	189901	11.2	4.72	29	1.5×10^{-2}	1.0×10^{-2} – 1.9×10^{-2}	–7.93	–7.93	2.23	74
NW Ascræus (northern flow)	1078601	11.6	4.21	33	—	—	–2.43	–2.43	1.49	98
W Ascræus	1756402	—	—	—	2.9×10^{-2}	2.3×10^{-2} – 3.5×10^{-2}	–15.7	–15.7	3.21	82
S Pavonis (northern flow)	1728801	—	—	—	6.2×10^{-3}	6.0×10^{-3} – 6.4×10^{-3}	–4.08	–4.08	1.08	95
S Pavonis (southern flow)	1728801	—	—	—	7.5×10^{-3}	5.5×10^{-3} – 9.4×10^{-3}	–3.38	–3.38	0.089	115

^aLoss tangent range (last column) is computed by using the 1 sigma fitting errors on the slope and computing loss tangent. The only track with flows that we could not derive a permittivity or loss tangent for is 1326501.

interface detection. Examples of these fits for tracks 1728801 northern and southern flows, 189901, and 1375301 can be found in Figure 4.

We calculated loss tangent values for nine subsurface interface detections in the Tharsis region (Table 1). Mean loss values ranged from 7.8×10^{-3} to 2.9×10^{-2} with an average of 1.0×10^{-2} . These values are consistent with terrestrial and lunar volcanic rocks, including basalts [Carrier et al., 1991]. Loss tangents in this range (0.007–0.03) imply a low to moderate concentration of radar wave absorbing minerals such as ilmenite, hematite, or magnetite. For two of the flows, 1078601 and 1326501, we were unable to derive meaningful loss tangents. This could potentially be caused by a rough subsurface in these locations, which could cause large amounts of scatter in the subsurface power measurements. The loss tangent measurements also produce more statistically meaningful results when the power is measured over a large range of depths; however, the depth range was similar for most flows.

The loss tangent measurements have both statistical noise as well as possible systematic uncertainty due to internal scattering. To address the statistical noise, we use the 1 sigma errors on the linear slope fit to compute a range of loss tangents for each fit. These are shown in Table 1. Scattering from within the flow, including from fractures and embedded lava textures or air gaps, can also contribute to a loss in echo power as the wave travels through the lava flow. Our derived loss tangents can be interpreted as an upper limit, because the scattering losses are unknown and will also contribute to the observed power loss with depth. Stillman and Grimm [2011] compute Born scattering models at SHARAD frequencies for plains subsurface reflectors and find attenuation rates of 0.014–0.27 dB/m for a permittivity of 4. This corresponds to scattering loss tangents of ~0.004–0.07. The high end of this range coincides with areas that have no SHARAD-detected subsurface reflections [Stillman and Grimm, 2011], and the scattering loss must be fairly low for the Tharsis area flows described here or we would not detect interfaces. The statistical and systematic uncertainties prevent us from determining whether the Tharsis area flows have differing compositions, but our derived range of values demonstrate that the flows have generally low microwave loss.

3. Geologic Discussion

SHARAD does not detect subsurface interfaces beneath distal flows far from the Tharsis volcanic summits and rift zones. In particular, we find no interfaces beneath flows east of Ascræus Mons and beyond Fortuna Fossae out to Echus Chasma (the region east of Figure 1). A majority

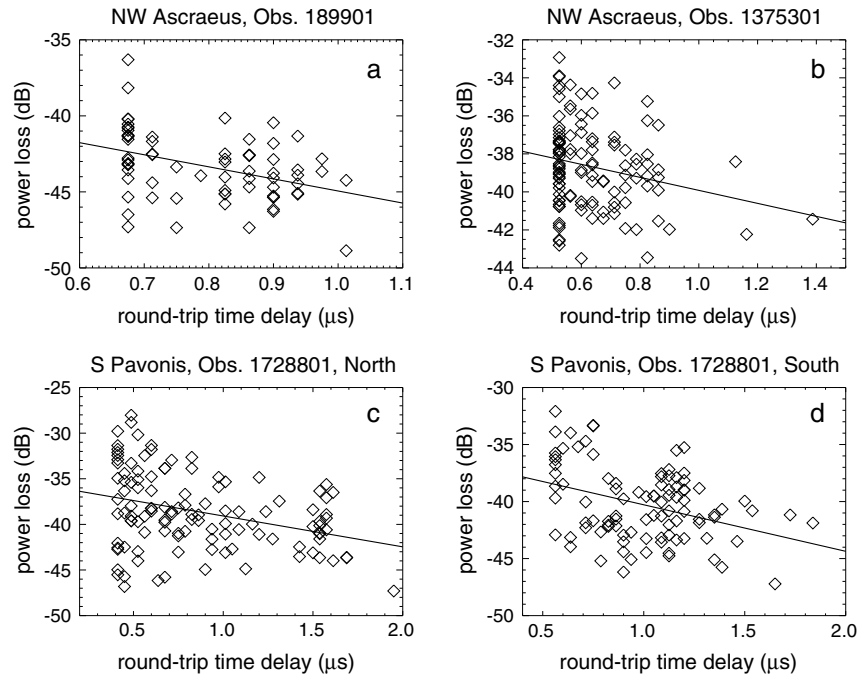


Figure 4. Round-trip time delay versus power loss for four flows. (a and b) Flows located northwest of Asraeus Mons and (c and d) flows located south of Pavonis Mons. The power versus depth data have varying degrees of scatter, but the loss tangent values computed for these flows fall well within the range measured for basalts.

of the flows with subsurface interfaces occur north and west of Asraeus Mons, with a few flows located near the Pavonis/Arsia rift zone.

There are multiple reasons SHARAD may detect interfaces beneath some flows but not others. First, the flows may have different compositions. It is possible that the original compositions were different, and SHARAD preferentially detects basal dielectric interfaces only beneath flows with low-loss tangents. It has also been noted that many SHARAD-detected interfaces occur in young terrains that date from very dry climate periods in Mars history [Stillman and Grimm, 2011]. For older lava flows that may have been subject to a wetter climate, small quantities of adsorbed water or minerals will increase the dielectric losses [Stillman and Grimm, 2011]. Such alteration of the original rocks could make the basal interface of the flows undetectable by SHARAD.

It is also possible that in this region SHARAD detects interfaces only in very flat areas where a significant layer of low-density material such as dust or regolith has accumulated. A low-density surface deposit would lower the permittivity contrast with the atmosphere and facilitates penetration of the radar wave into the surface, while exposed rocky deposits would reflect more power and thus allow less of the sounder signal to reach a basal interface. A simple model of transmission through dielectric layers can be used to demonstrate this effect. Transmission into the surface at nadir incidence is

$$T = 1 - \left(\frac{\sqrt{\epsilon_2'} - \sqrt{\epsilon_1'}}{\sqrt{\epsilon_2'} + \sqrt{\epsilon_1'}} \right)^2 \quad (3)$$

where ϵ_1' and ϵ_2' are the permittivity values of the top and bottom layers, respectively. The round-trip attenuation upon passage through a layer can be written as [Campbell, 2002]

$$A = \exp(-4\alpha h); \quad \alpha = \frac{2\pi}{\lambda} \left[\frac{\epsilon'}{2} \left(\sqrt{1 + \tan^2 \delta} - 1 \right) \right]^{1/2} \quad (4)$$

where h is the thickness of the layer and ϵ' is the permittivity of the layer. Figure 5 shows the total round-trip transmission and attenuation for mantling deposits with $\epsilon' = 2$ and varying thicknesses and loss tangents overlying a lava flow with $\epsilon' = 9$. Transmission is shown relative to that of a bare, unmantled lava flow. Meter-

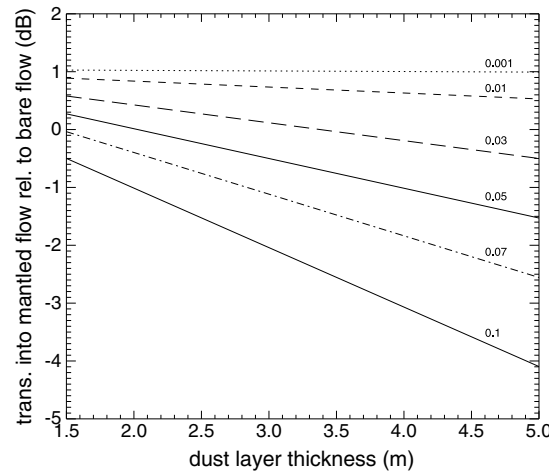


Figure 5. Total round-trip signal transmission and attenuation into a mantled lava flow relative to an unmantled lava flow, in dB. The plot provides a comparison of mantling dust layers with varying thicknesses (x axis) and loss tangents (loss tangent value marked on the right side of each plot line). The plot lines were calculated using a mantling layer with $\epsilon' = 2$ and a lava flow with $\epsilon' = 9$. Positive values indicate that transmission is increased due to the presence of the mantling layer.

[2012]. The radar-dark Tharsis flows have reflectivities from -15 to -18 dB, and the radar-bright flows have reflectivities from -6.1 to -9.2 dB, corresponding to a 6–12 dB difference in reflectivity at a normalized incidence angle of 30° [Harmon *et al.* 2012]. Assuming a model with an upper dust layer with $\epsilon' = 2$ covering a lava flow with $\epsilon' = 9$, we can compare the reflected signal from a mantled lava flow to that of an unmantled flow:

$$f = \frac{\text{reflection from mantled flow}}{\text{reflection from bare lava flow}} \cong 2AT^2R_e \quad (5)$$

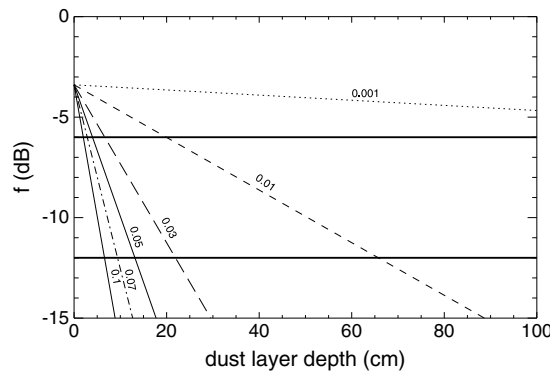


Figure 6. The reflected power from a mantled surface relative to the reflected power from an unmantled surface (equation (5)) for multiple loss tangents (thin lines, loss tangent marked). In the Ascreaus Mons area, differences in reflectivity between bright and dark flows are 6–12 dB [Harmon *et al.* 2012]; this boundary is marked on the plot with solid thick lines. For a range of loss tangents, dust layers of ~ 10 – 60 cm can suppress the reflectivity by the amounts measured by Harmon *et al.* [2012]. In the case of very low loss dust layers, a couple meters of dust is needed to suppress the S-band (12.6 cm wavelength) reflectivity by 12 dB.

scale layers of low-density (1 – 2 g/cm³), low-loss (<0.05) dust can increase the transmission into the lava flow relative to an unmantled surface.

Earth-based radar measurements at 12.6 cm wavelength (S band) can provide an additional test of this hypothesis [Harmon *et al.*, 2012]. These shorter-wavelength signals penetrate no more than a few meters into the surface. In the Tharsis region, the Earth-based radar image shows a variety of flow textures. Some are radar bright, indicative of a rough surface, while other areas of the flows are radar dark. These dark regions are interpreted by Harmon *et al.* [2012] to be covered in smooth mantling deposits. In the radar-bright area east of Tharsis, SHARAD does not detect any basal interfaces. The flow interfaces detected by SHARAD are instead concentrated in radar-dark regions, suggesting that SHARAD may well preferentially detect flows in regions covered by at least a thin layer of dust.

We can again use transmission models to assess whether mantling layers can explain the reflectivity difference observed by Harmon *et al.*

where A is the round-trip attenuation from equation (4), T is the loss from transmission through the surface/mantle interface, and R_e is the effective reflectivity of the buried interface relative to its reflectivity in free space. The transmission coefficients ($1/R$) at 30° incidence into the dust layer are high, e.g., ~ 0.95 , and the ratio of reflection coefficients for a mantled versus unmantled lava flow surface at 30° incidence is about $R_e = 0.5$. Figure 6 illustrates how mantling layers with different thicknesses and loss tangents affect the total backscatter cross section of the surface. To decrease the reflectivity by 6–12 dB, dust layers of ~ 10 – 60 cm are needed for loss tangents between 0.01 and 0.1. However, for very low loss dust layers (0.001–0.01), meters of dust are required to reduce the reflectivity by the Harmon *et al.* [2012] amounts. Low-loss meter-thick dust layers would also substantially improve the SHARAD penetration into the buried flows (Figure 5). SHARAD detects subsurface interfaces

beneath some bright flows mapped in *Harmon et al.* [2012] (e.g., west Tharsis [*Carter et al.*, 2011; *Stillman and Grimm*, 2011]), so thick mantling layers are not always required for detection of subsurface interfaces in volcanic areas, but in this area of Tharsis dust mantling almost certainly contributes to the observed radar scattering behavior.

SHARAD will also not detect interfaces in areas where lava flows are stacked in sequence with minimal density contrast. There is abundant evidence for pyroclastic volcanism during the development of the Tharsis area [*Mouginis-Mark*, 2002; *Brož and Hauber* 2012], including the deposition of the MFF, which overlays Tharsis volcanic flows that traveled west onto the plains [*Fuller and Head* 2002]. These episodes of tephra deposition interspersed with effusive lavas would have created stratigraphic sequences with density changes visible to radar sounding. The flows around Fortuna Fossae and east to Echus Chasma may have been too distant from, or upwind of, the sites of pyroclastic activity. Alternatively, in many locations a stack of flows several tens to hundreds of meters thick (i.e., too thick to penetrate with SHARAD) may have formed in succession over a time period with no intervening dust or ash deposition.

In areas where SHARAD detects flow basal interfaces, we sometimes detect interfaces between different stratigraphic layers. Northwest of Ascræus Mons, we clearly see through the upper layer of lava flows, but in cases like track 1375301 (Figure 1) we also see through a deeper interface. This portion of track 1375301 is located between two flows that lie on top of flat terrain. Based on superposition, we know that these flows are younger than the surrounding terrain, yet we see an interface located directly under the flat terrain. This indicates SHARAD-detected interfaces at different terrain depths and is able to record multiple episodes of lava flows. This is similar to what we find in western Tharsis [*Carter et al.*, 2011] and the Elysium region [*Morgan et al.*, 2013].

While most of the flows we identified have flat subsurface interfaces, in the region south of Pavonis we detect an apparently concave subsurface reflector (Figure 3). This shape indicates preexisting topography that was either circular (e.g., a buried crater) or cylindrical (e.g., a buried channel). Tracks slightly to either side did not reveal the same feature, so we are unable to trace how far this subsurface feature might extend.

4. Conclusions

The SHARAD sounding radar survey of Tharsis shows that radar-detected basal flow interfaces are primarily associated with rift zone volcanism on flat, dust-covered terrain. The permittivity and loss tangent values calculated for the flows northwest and west of Ascræus Mons, and south of Pavonis Mons, are consistent with laboratory-measured values for terrestrial and (low- to moderate-titanium) lunar basalts. Although it is not possible to determine whether the SHARAD-detected flows have a different composition from other flows, greater dust cover, or a more contrasting dielectric interface, it is clear that Tharsis rift zone volcanism produced flows with fairly similar bulk densities and loss tangents.

The results presented here and preliminary work for western Tharsis [*Carter et al.*, 2011] also demonstrate that there are clear differences in SHARAD-detected interfaces between Tharsis and the Elysium region. In the Tharsis region, we do not see stacked interfaces at different depths, but these are typical in the Elysium region [*Morgan et al.*, 2013]. The Elysium region has outflow channels carved by groundwater releases [*Morgan et al.*, 2013]. One possibility is that the groundwater deposited low-density sediments that contrast with the lava, making detection of stacked interfaces more probable. In the Tharsis region, however, lava may frequently have been deposited on top of other lava, leading to a smaller likelihood of multiple layer detection. Future work with numerical modeling and terrestrial analog studies, or rover-based ground-penetrating radar, could help to determine if stacked interfaces are present in the Elysium region but not at Tharsis.

References

- Baloga, S. M., and L. S. Glaze (2008), A self-replication model for long channelized lava flows on the Mars plains, *J. Geophys. Res.*, *113*, E05003, doi:10.1029/2007JE002954.
- Baloga, S. M., P. J. Mouginis-Mark, and L. S. Glaze (2003), Rheology of a long lava flow at Pavonis Mons, Mars, *J. Geophys. Res.*, *108*(E7), 5066, doi:10.1029/2002JE001981
- Bleacher, J. E., R. Greeley, D. A. Williams, S. C. Werner, E. Hauber, and G. Neukum (2007), Olympus Mons, Mars: Inferred changes in late Amazonian aged effusive activity from lava flow mapping of Mars Express High Resolution Stereo Camera data, *J. Geophys. Res.*, *112*, E04003, doi:10.1029/2006JE002826.

Acknowledgments

Funding for this project was provided by the NASA Undergraduate Student Research Program and by the NASA MRO project. SHARAD was contributed by the Italian Space Agency; we thank Principle Investigator Roberto Seu and the SHARAD operations team for their efforts in acquiring this data. The SHARAD data were processed at the Smithsonian Institution and Southwest Research Institute in Boulder, CO. They are also available through the NASA Planetary Data System.

- Brož, P., and E. Hauber (2012), A unique volcanic field in Tharsis, Mars: Pyroclastic cones as evidence of explosive eruptions, *Icarus*, *218*, 88–99, doi:10.1016/j.icarus.2011.11.030.
- Campbell, M. J., and J. Ulrichs (1969), Electrical properties of rocks and their significance for lunar radar observations, *J. Geophys. Res.*, *74*, 5867–5881, doi:10.1029/JB074i025p05867.
- Campbell, B. A. (2002), *Radar Remote Sensing of Planetary Surfaces*, Cambridge Univ. Press, Cambridge, U. K.
- Campbell, B. A., L. M. Carter, R. J. Phillips, N. E. Putzig, J. J. Plaut, A. Safaeinili, R. Seu, D. Biccari, A. Egan, and R. Orosei (2008), SHARAD radar sounding of the Vastitas Borealis Formation in Amazonis Planitia, *J. Geophys. Res.*, *113*, E12010, doi:10.1029/2008JE003177.
- Carrier, W. D., G. R. Ohloeft, and W. Mendell (1991), Physical properties of the lunar surface, in *Lunar Sourcebook*, pp. 457–567, Cambridge Univ. Press, New York.
- Carter, L. M., B. A. Campbell, J. W. Holt, R. J. Phillips, N. E. Putzig, S. Mattei, R. Seu, C. H. Okubo, and A. F. Egan (2009a), Dielectric properties of lava flows west of Ascraeus Mons, Mars, *Geophys. Res. Lett.*, *36*, L23204, doi:10.1029/2009GL041234.
- Carter, L. M., et al. (2009b), Shallow radar (SHARAD) sounding observations of the Medusae Fossae Formation, Mars, *Icarus*, *199*, doi:10.1016/j.icarus.2008.10.007.
- Carter, L. M., B. A. Campbell, G. A. Morgan, R. J. Phillips, J. J. Plaut, N. E. Putzig, and A. F. Egan (2011), Mapping subsurface interfaces in eastern Amazonis Planitia using SHARAD data, EPSC-DPS Joint Meeting 2011, p. 1187, Nantes, France.
- Fuller, E. R., and J. W. Head (2002), Amazonis Planitia: The role of geologically recent volcanism and sedimentation in the formation of the smoothest plains on Mars, *J. Geophys. Res.*, *107*(E10), 5081, doi:10.1029/2002JE001842.
- Glaze, L. S., and S. M. Baloga (2006), Rheologic inferences from the levees of lava flows on Mars, *J. Geophys. Res.*, *111*, E09006, doi:10.1029/2005JE003278.
- Glaze, L. S., S. M. Baloga, W. B. Garry, S. A. Fagents, and C. Parcheta (2009), A hybrid model for leveed lava flows: Implications for eruption styles on Mars, *J. Geophys. Res.*, *114*, E07001, doi:10.1029/2008JE003278.
- Harmon, J. K., M. C. Nolan, D. I. Husmann, and B. A. Campbell (2012), Arecibo radar imagery of Mars: The major volcanic provinces, *Icarus*, *220*, 990–1030, doi:10.1016/j.icarus.2012.06.030.
- Heggy, E., P. Paillou, G. Ruffie, J. M. Malezieux, F. Costard, and G. Grandjean (2001), On water detection in the Martian subsurface using sounding radar, *Icarus*, *154*, 244–257, doi:10.1006/icar.2001.6717.
- Holt, J. W., M. E. Peters, S. D. Kempf, D. L. Morse, and D. D. Blankenship (2006), Echo source discrimination in single-pass airborne radar sounding data from the Dry Valleys, Antarctica: Implications for orbital sounding of Mars, *J. Geophys. Res.*, *111*, E06S24, doi:10.1029/2005JE002525.
- Morgan, G. A., B. A. Campbell, L. M. Carter, and J. J. Plaut (2013), 3D visualization of the internal structure of the youngest volcanic plain on Mars, Lunar and Planetary Science Conference 2013, Houston, Tex., Abstract #2640.
- Mouginis-Mark, P. J. (2002), Prodigious ash deposits near the summit of Arsia Mons volcano, Mars, *Geophys. Res. Lett.*, *29*(16), doi:10.1029/2002GL015296.
- Seu, R., D. Biccari, R. Orosei, L. V. Lorenzoni, R. J. Phillips, L. Marinangeli, G. Picardi, A. Masdea, and E. Zampolini (2004), SHARAD: The MRO 2005 shallow radar, *Planet. Space Sci.*, *52*, 157–166, doi:10.1016/j.pss.2003.08.024.
- Seu, R., et al. (2007), SHARAD sounding radar on the Mars Reconnaissance Orbiter, *J. Geophys. Res.*, *112*, E05S05, doi:10.1029/2006JE002745.
- Stillman, D. E., and R. E. Grimm (2011), Radar penetrates only the youngest geological units on Mars, *J. Geophys. Res.*, *116*, E03001, doi:10.1029/2010JE003661.
- Ulaby, F. T., T. Bengal, J. East, M. C. Dobson, J. Garvin, and D. Evans (1988), Microwave dielectric spectrum of rocks, *Rep. 23817-1-T*, Univ. of Mich. Radiat. Lab., Ann Arbor.
- Watters, T. R., et al. (2007), Radar sounding of the Medusae Fossae Formation Mars: Equatorial ice or dry, low-density deposits, *Science*, *318*, 1125–1128.